

Original article

Using proper orthogonal decomposition to solve heat transfer process in a flat tube bank fin heat exchanger

Ye Wang^{1,2*}, Xintong Xia¹, Yi Wang³, Liangbi Wang², Wenting Hu¹

¹*School of Environmental and Municipal Engineering, Lanzhou Jiaotong University, Lanzhou 730070, P. R. China*

²*Key Laboratory of Railway Vehicle Thermal Engineering, Ministry of Education of China, Lanzhou 730070, P. R. China*

³*National Engineering Laboratory for Pipeline Safety/MOE Key Laboratory of Petroleum Engineering/Beijing Key Laboratory of Urban Oil and Gas Distribution Technology, China University of Petroleum, Beijing 102249, P. R. China*

(Received November 20, 2017; revised December 3, 2017; accepted December 5, 2017; published December 25, 2017)

Abstract: Proper orthogonal decomposition (POD) reduced-order model can save computing time by reducing the dimension of physical problems and reconstructing physical fields. It is especially suitable for large-scale complex problems in engineering, such as ground heat utilization, sea energy development, mineral exploitation, multiphase flow and flow and heat transfer with complex structure. In this paper, the POD reduced-order model was used to calculate the heat transfer in a flat tube bank fin heat exchanger. The calculating results of the finite volume method (FVM) were adopted as the snapshot samples. SVD method was used to decompose the samples to obtain a series of bases and corresponding coefficients on sampling conditions. With these coefficients, interpolation method was used to calculate the coefficients on predicting conditions. And the physical field has been reconstructed using the bases and the interpolated coefficients directly.

In the calculation of heat transfer unit of flat tube fin heat exchanger, air-side Reynolds number, transverse tube spacing and the fin spacing were chosen as the variables. The results obtained by the POD method are in good agreement with the results calculated by the FVM. Moreover, the POD reduced-order model presented in this paper is more advantageous in comparison with the FVM in terms of accuracy, suitability, and computational speed.

Keywords: Proper orthogonal decomposition (POD), POD reduced-order model, flat tube bank fin heat exchanger, interpolation method, reconstructed temperature field.

Citation: Wang, Y., Xia, X., Wang, Y., et al. Using proper orthogonal decomposition to solve heat transfer process in a flat tube bank fin heat exchanger. *Adv. Geo-energ. Res.* 2017, 1(3): 158-170, doi: 10.26804/ager.2017.03.03.

1. Introduction

Tube-fin heat exchangers are employed in a wide variety of engineering applications as a universal device in heat transfer process, such as vehicles (Bellocchi et al., 2018), cooling systems (Sivasakthivel et al., 2017), air conditioning (Miseviciute et al., 2018), chemical engineering, aerospace, electronic chip cooling and power systems (Song et al., 2017). The air side heat resistance of the heat exchanger dominates the thermal resistance of the whole system and plays a decisive role in the heat transfer efficiency (Jacobi and Shah, 1998). For the requirements the consistency of "heat transfer capacity, volume, energy consumption" of the heat exchanger in the industrial application, the tube spacing (Wang et al., 2010;

Song et al., 2011; Wang et al., 2018), fin spacing (Hu et al., 2013; 2015), fin material (Lizardi et al., 2004; Gai et al., 2010), fin structure (Han et al., 2013; Lin et al., 2014; 2015; Arora et al., 2015; Wei et al., 2016; Capata and Beyene, 2017; Guo et al., 2017; Agbossou et al., 2018), fluid flow parameters (Wang et al., 2012a; Lin et al., 2014) and other aspects of the heat exchanger heat transfer performance were studied. The heat transfer performance of the fin with vortex generators (VGs) punched on the fin surface also be studied (Wang et al., 2010; Aliabdi et al., 2016; Dezan et al., 2016; Salviano et al., 2016; Väälikangas et al., 2018). When the area goodness factor was used as the criteria on the condition of one tube unit of heat exchanger for commonly used fin materials and fin thickness, the transversal tube pitch has considerable effect on the heat

*Correspondent author. Email: wangye@mail.lzjtu.cn

transfer enhancement of VGs.

To study the heat transfer performance of heat exchanger with complex structure by experimental test will inevitably consume a lot of money and time, but also, the detail characteristics of the flow field and the temperature field cannot be captured. However, fast numerical simulation method can greatly reduce the design costs. The finite volume method is often used to solve the inherent characteristics of the iterative process. In order to obtain the detailed information of the flow field and the temperature field, millions of grids must be discreted, which means advanced computer and a lot of computing time.

POD is an efficient method which can extract characteristic samples from a large set of data and can combine with interpolation method to reconstruct complex problems by establishing the reduced-order model (ROM). The reduced-order model of POD method can reduce the degrees of freedom of a problem and reduce the calculation time substantially (Wang et al., 2012b). Therefore, POD method has become one of the hotspots in the field of numerical calculation of flow and heat transfer and it has been widely used to analyze practical problems.

POD was firstly proposed by Pearson in 1901 (Pearson, 1901). It is based on the numerical solution to construct a linear system rather than directly linearize the control equations with a good processing power for both linear and nonlinear problems, so it is continuously studied and applied in many fields, such as singular value analysis and sample identification (Fukunaga, 1990), statistics (Jolliffe, 2002; Aquino, 2007), image processing (Rosenfeld, 1982), meteorological science (Kylikof, 1988; Majda et al., 2003), ocean numerical simulation (Crommelin and Majda, 2004; Luo et al., 2007), turbulent drag-reducing flow (Lumley, 1967; Cazemier et al., 1998; Wang et al., 2011; Wang et al., 2012c), mobile heat transfer (Jolliffe, 2002). "Snapshot" method was proposed by Sirovich (Sirovich, 1987) in 1987. The time-dependent matrix is calculated instead of the spatial covariance matrix to solve the basis functions, which saves the storage space and computing time greatly. Li et al. (2011) deduced a simplified finite element scheme for the parabolic problem with the POD basis function, analyzed the error between the usual finite element scheme and finite element format simplified with POD basis function and proposed a POD-Galerkin model based on finite element method to analyze the mass transfer problem in soil.

The POD technique has been widely used in the study of heat and mass transfer (Wang et al., 2012d). Mahapatra et al. (2016) used the POD to assess the energy content of buoyancy-driven flow in an air-filled enclosure under different Ra numbers and switching frequencies. POD was also adopted to understand the flow dynamics information about the coherent structures of different energy modes. Polansky and Wang (2017) utilized the POD to identify flow structure and revealed the air-water flow regimes in a horizontal pipeline with slag, plug and wavy stratified phenomena. Zhang and Xiang (2015) proposed an efficient method based on POD to resolve the transient heat conduction problems with enough computational accuracy. Brenner et al. (2012) used

the reduced-order model based on POD to study the non-isothermal flow using numerical results from a full-order computational fluid dynamics model. The results show that both the reduced-order and full-order models can solve the problem with high accuracy. Puragliesi and Leriche (2012) obtained the fundamental velocity and temperature coherent structures in the fully confined cubical three-dimensional differentially heated cavity flow by using POD. Singer and Green (2009) proposed an adaptive POD method to reduce the computational cost of reacting flow simulations. The method was applied to a one-dimensional, laminar premixed CH_4 -air flame with errors less than 0.25% and a speed-up factor of 3.5. Yang et al. (2014) investigated the mechanism of convective heat transfer enhancement in a turbulent flow of nanofluid by POD analysis. The results indicate that turbulent energy contributions from the first few eigenmodes are reduced by adding nanoparticles and the overall energy distribution becomes more uniform among coherent structures in the fluctuating temperature field.

POD have been used in the field of earth energy in recently years. Mudunuru et al. (2017) assessed the utility of regression-based reduced-order models (ROMs) developed from high-fidelity numerical simulations for predicting transient thermal power output for an enhanced geothermal reservoir while explicitly accounting for uncertainties in the subsurface system and site-specific details. The proposed regression-based ROMs is attractive for real-time EGS applications because they are fast and provide reasonably good predictions for thermal power output. Cao et al. (2006) made an initial effort to investigate problems related to POD reduced modeling of a large-scale upper ocean circulation in the tropic pacific domain, which showed that POD is an efficient model of reduction technique for simulating physical process governed by partial differential equations. Atam and Helsen (2016) proposed a compact overview of the state-of-the-art in modeling of ground-coupled heat pump (GCHP) systems and an in-depth review of their optimal control with the associated research challenges. The main focus is on optimal control but since design of an optimal controller may require a model, POD reduced-order model is expected to be applied to study such problems. Chen et al. (2015) proposed a singular value decomposition program on a MATLAB platform to extract deeply buried geological information reflecting deep-seated geological structures and the concealed granites by decomposing gravity signals within the Gejiu tin polymetallic ore field. Li et al. (2013) developed a numerical optimization methodology of ventilation system operation to improve indoor environment quality and energy costs for space heating and cooling simultaneously by POD reduced-order model, which indicates that the present optimization approach is able to improve indoor comfort and energy costs of ventilation system in a balanced way. Han et al. (2015) proposed a POD Galerkin reduced-order model for unsteady-state heat conduction problems based on body-fitted coordinate. The conclusion shows that the reduced-order model has great engineering application value and would be a very helpful tool to solve the time-consuming and energy saving problem involved in the optimal design and risk assessment of oil pipeline. In addition, the POD is promising to facilitate analysis data and predict the

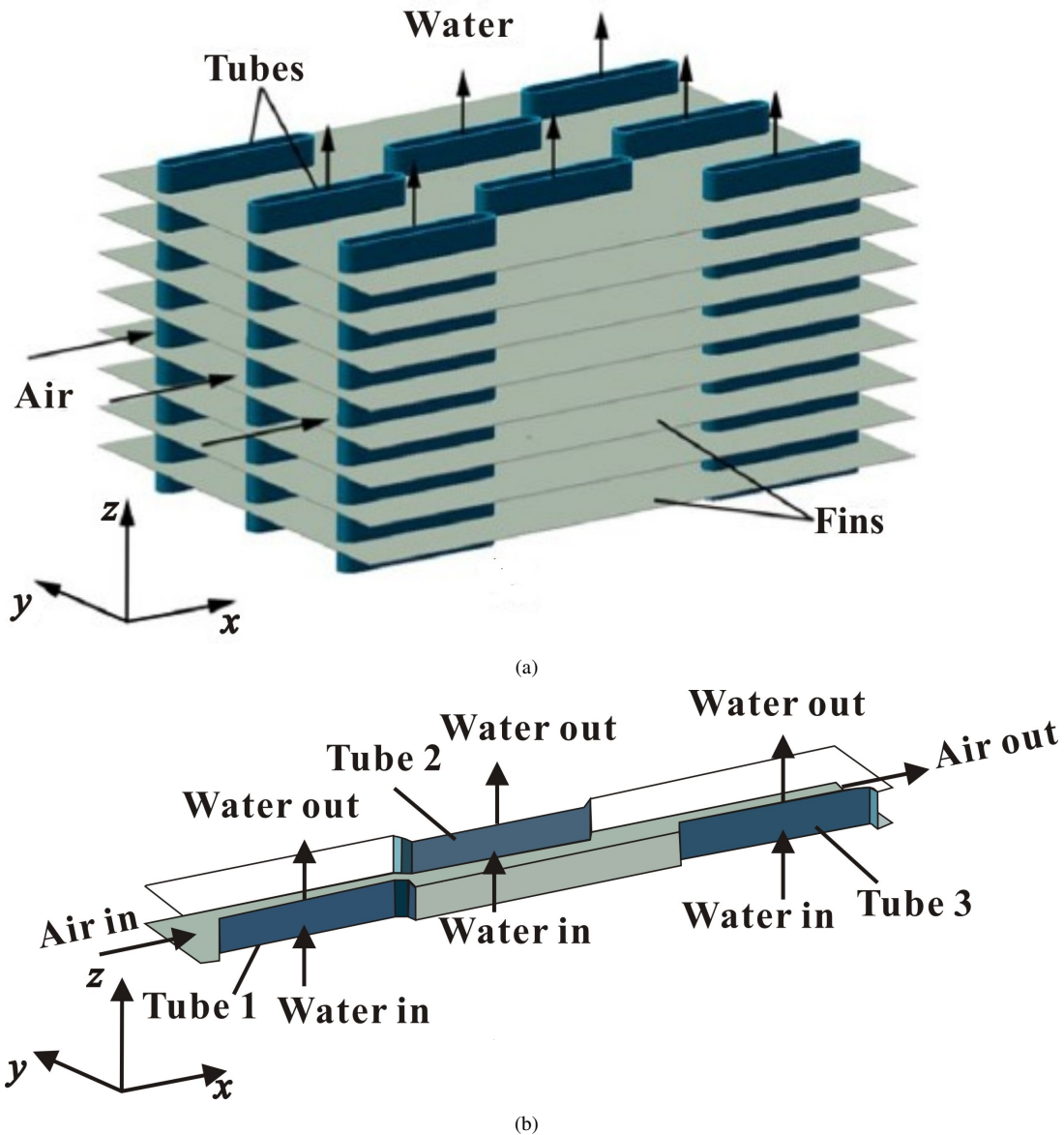


Fig. 1. Physical model of flat tube bank fin heat exchanger.

variation of the water level and topographic position (Nair, 2017).

POD are also used in the study of heat exchanger. Ding and Tao (2011) applied a reduced-order model of POD interpolation to a simple tube fin heat exchanger. The POD model was established by linear interpolation in 21 groups of velocity field and temperature field at Reynolds number in the range of 100 ~ 2000. The results were in good agreement with that of the SIMPLE algorithm, but the calculation time was only 1/1200 of the SIMPLE algorithm. Their research showed the potential of POD methods in complex geometric regions.

However, most of the studies related to POD model are only for simple geometric regions. Using both POD interpolation method and POD projection method in flow and heat transfer calculations of the flat tube heat exchanger has not been reported. In this paper, a high-efficiency POD reduced-order model is proposed and applied to the flow and heat

transfer in a flat tube bank fin heat exchanger. Different reduced-order models are established by interpolation methods based on the general control equation of flow and heat transfer. The POD interpolation method under unstructured grid and three-dimensional body coordinates are studied. The accuracy, speed and robustness of different POD interpolation reduced-order models are studied and a high-efficiency POD reduced-order model in good agreement with that of FVM for complex geometric region is established.

2. Physical model and numerical method

2.1 Physical model and assumptions

Physical description and parameters of flat tube bank fin heat exchanger are depicted schematically in Fig. 1. It consists of a large number of parallel tubes and numerous plain fins

typically. Tubes are located in staggered manner. In the study, water flows through the tubes and gas flows through the channel formed by the tubes and the fins. And the hot water can be cooled by air through conjugate heat transfer. As shown in Fig. 1(b), the computational domain of the three-rows staggered flat tube bank fin heat exchanger is composed of four parts, they are air channel, fins, tubes and water channel.

The flat tube bank fin heat exchanger in three-dimensional is shown in Fig. 1(a), a heat transfer unit is selected to study, as shown in Fig. 1(b). Since the size of the air flow unit is closely related to the geometrical dimensions of the fins, according to the operable geometric dimension changing structure of the similar flat tube bank fin heat exchanger (Liu et al., 2008), the effect of the geometric size on the heat transfer process was observed by changing the transverse tube spacing (S_1) and the fin spacing (T_p). The related parameters are shown in Table 1, $S_1 = 16 \text{ mm}$, $T_p = 2.0 \text{ mm}$, $a = 2.5 \text{ mm}$, $S_2 = 22 \text{ mm}$ and $b = 18.0 \text{ mm}$ are originated from the real dimension of the locomotive radiator. The remaining values are given by the authors for research purpose. In Fig. 1(b), T_p is the vertical distance between the upper surface of the lower fin and the lower surface of the upper fin.

Table 1. Heat dissipation unit geometry.

Parameters	Parameter value (mm)		
	1	2	3
S_1	12.8	16	21.2
T_p	1.6	2.0	2.4
a		2.5	
S_2		22	
b		8.5	

The specific geometric parameters of heat exchanger unit are shown in Fig. 2.

2.2 Boundary conditions

For the studied heat transfer unit in this paper, the walls of tubes and fin thickness are ignored. In practical problems, the pipe walls and fin surfaces are non-isothermal wall temperature conditions. However, in this paper, we focus on the comparison of POD reduced-order model with traditional FVM in terms of computational efficiency and accuracy. Therefore, in order to simplify the calculation, the tube walls and fin surfaces are set to isothermal wall temperature boundary condition. The air inlet velocity varies with the operating conditions and the outlet flow is assumed to be no backflow (Wang et al., 2012a). The mathematical descriptions of the air side boundary conditions are given as follows. Previous studies have already ensured the reliability of the boundary conditions in this study.

(1) entrance boundary

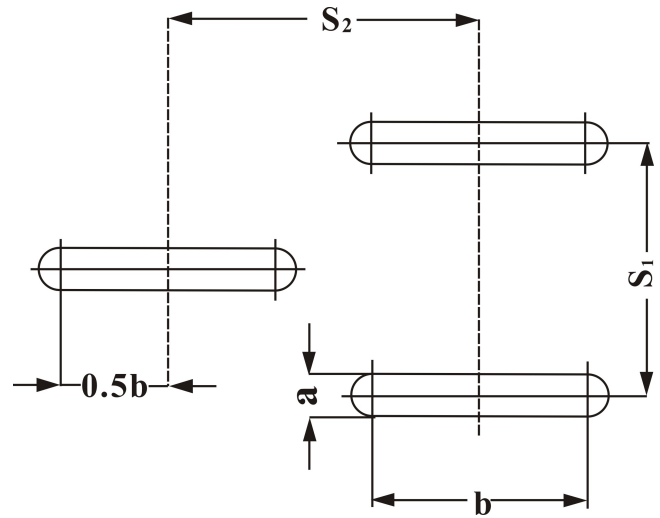


Fig. 2. Heat exchanger unit size parameter.

The average flow rate and average temperature of the inlet part AA' J' J are given as equation (1).

$$u(0, y, z) = u_{in}, v(0, y, z) = 0, w(0, y, z) = 0, \quad (1)$$

$$T(0, y, z) = T_{in}$$

where u_{in} depends on the inlet flow rate condition, $T_{in} = 40^\circ\text{C}$.

(2) outlet cross section boundary

The velocity boundary of the outlet section DEE'D' of the airflow channel is defined as equation (2).

$$\partial u(L_x, y, z) / \partial x = 0, \partial v(L_x, y, z) / \partial x = 0, \quad (2)$$

$$\partial w(L_x, y, z) / \partial x = 0$$

The remaining sub-velocities and the temperature boundary conditions of the outlet section are defined as equation (3).

$$\partial v(L_x, y, z) / \partial x = 0, \partial w(L_x, y, z) / \partial x = 0, \quad (3)$$

$$\partial T(L_x, y, z) / \partial x = 0$$

(3) side wall region 1

In Fig. 3, the symmetry planes JII'J', GG'H', FEE'F', ABB'A' and CDD'C', $v(0, y, z) = 0$, the other two sub-speeds and the temperature are defined in equation (4) and (5).

$$\partial u(x, 0, z) / \partial y = 0, \partial w(x, 0, z) / \partial y = 0, \partial T(x, 0, z) / \partial y = 0 \quad (4)$$

$$\partial u(x, S_1/2, z) / \partial y = 0, \partial w(x, S_1/2, z) / \partial y = 0, \quad (5)$$

$$\partial T(x, S_1/2, z) / \partial y = 0$$

(4) side wall region 2

The boundary conditions of interface between the air and the pipe walls of the air side, I'HH' and G'GFF' as shown in Fig. 3 are given in equation (6).

$$T(x, y, z)|_a = T_{fin} \quad (6)$$

$$T_{fin} = 88^\circ\text{C}$$

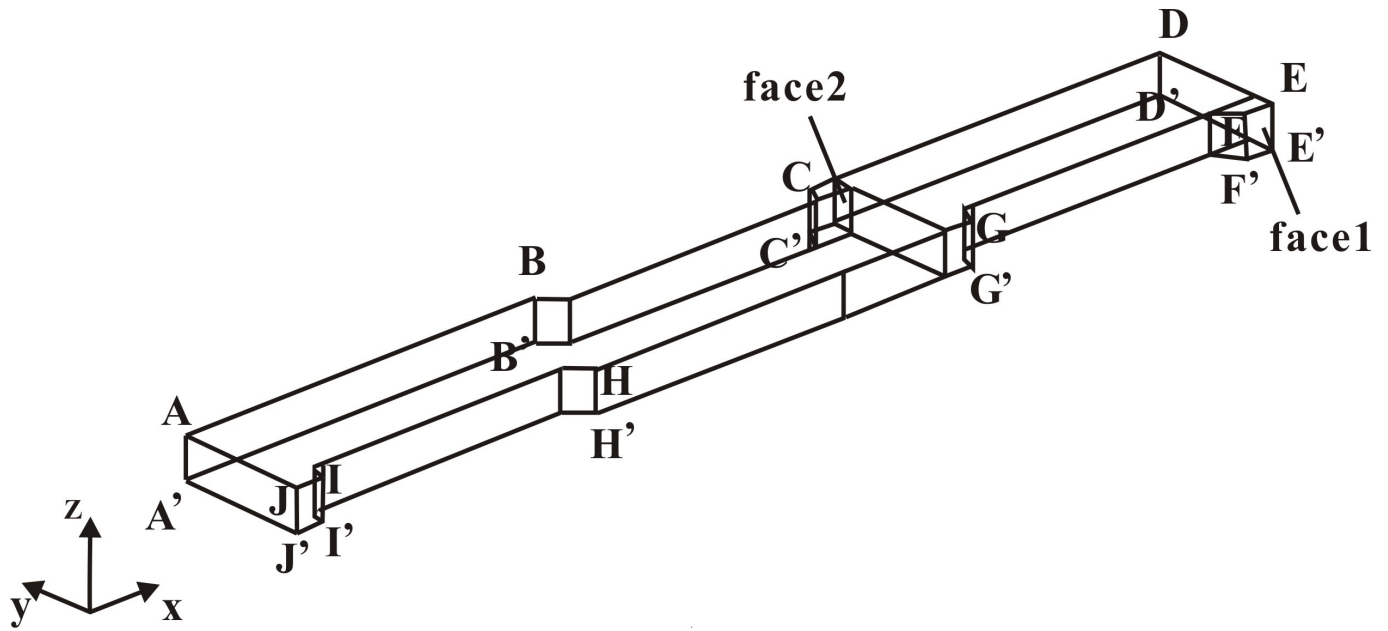


Fig. 3. Air flow channel and boundary definition.

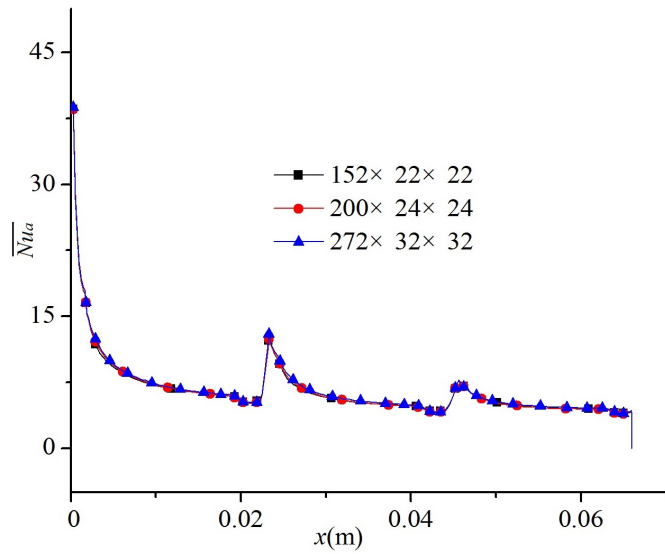


Fig. 4. Grid independence verification.

(5) top and bottom surface

The boundary conditions of the interface between air and fin, ABCDEFGH IJA and A'B'C'D'E'F'G'H'I'J'A' are defined in equation (7).

$$T(x, y, z)|_{L_z} = T_{fin}, T(x, y, z)|_0 = T_{fin} \quad (7)$$

In addition, face 2 has the same boundary condition as face 1.

2.3 Grid independence verification

Three sets of grids are constructed in the model region of Fig. 3, 152*22*22, 200*24*24 and 272*32*32. Considering

the high gradient variation of parameters in the boundary layer, in order to reduce the difference during the information transfer resulting from the skewed grids in the transitional regions of the boundaries, the Poisson differential equation method is employed to modify the grid system generated by algebraic method. But also, the grid density is locally refined in the region close to the interface between the fluid and the solid. The convective heat transfer of the fin unit is calculated under the condition of $T_p = 3.2 \text{ mm}$, $S_1 = 16 \text{ mm}$ and $Re_a = 1100$. The span-wise average Nusselt (Nu) number along main flow direction is shown in Fig. 4. It can be seen that the influence of the grid size on the results is small. The grid of $272 * 32 * 32$ is adopted as the grid number in this paper.

2.4 Numerical method verification

In order to verify the reliability of the numerical method, the model with the experimental geometric parameters is generated. And the numerical results and the experimental results of the Nu number (\overline{Nu}_a) and the friction factor (f_a) are compared. In this paper, the numerical method is checked by the experimental empirical equation in reference (Kylikof, 1988).

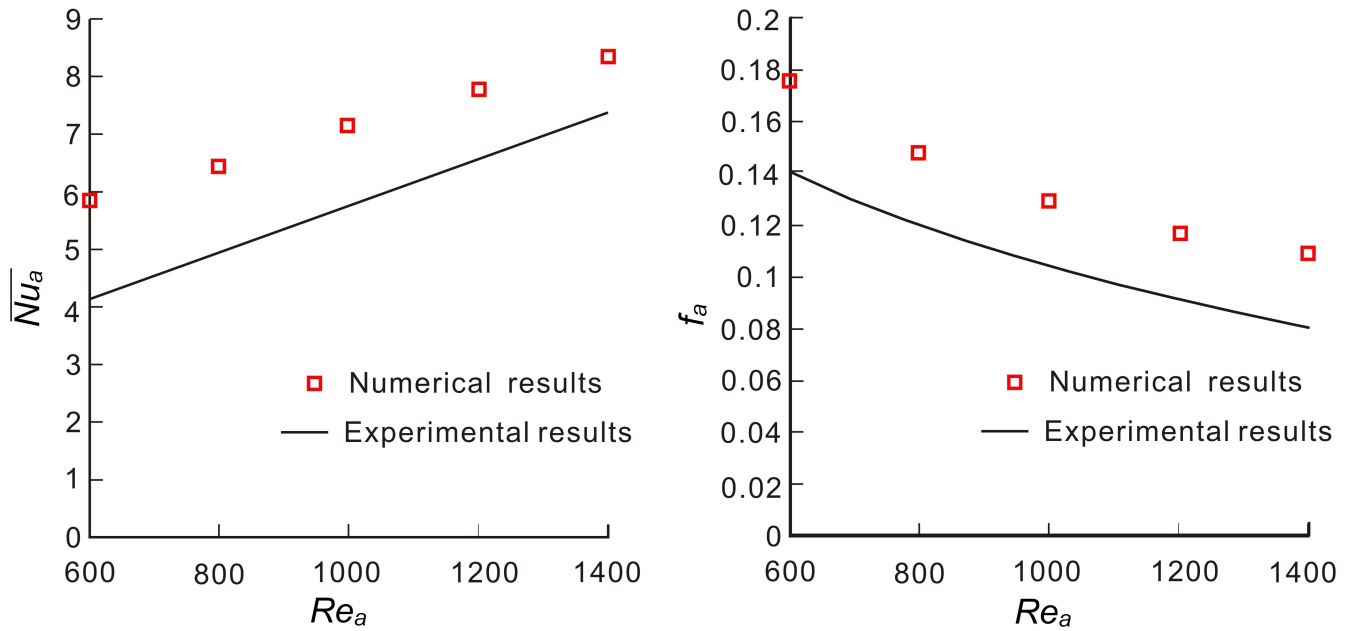
$$\overline{Nu}_a = 0.072 Re_a^{0.695} Pr^{0.33} \left(\frac{a}{T_p}\right)^{-0.54} \left(\frac{S_1 - a}{2T_p}\right)^{-0.14} \quad (8)$$

($Re_a = 400 \sim 20000$)

$$f_a = 8.35 Re_a^{-0.627} (a/d_e)^{0.3} \varepsilon_\lambda, \quad \varepsilon_\lambda = 1.65^{(\lg Re_a)^{-2.53}} \quad (9)$$

($Re_a = 400 \sim 20000$)

$$Re_a = \rho u_{\max} d_e / \mu \quad (10)$$



(a) Comparison of average Nu with the experimental results

(b) Comparison of (f_a) with the experimental results

Fig. 5. Numerical method verification.

$$Ra = Pr \times Gr = \frac{g\beta L^3 \Delta T}{\nu\alpha} \quad (11)$$

Fig. 5(a) shows the comparison of the average Nu number on the air side under the same condition as in reference. It can be seen that the average Nu number increases with the increasing Reynolds number. The relative error of the numerical results and the experiments results decreases with the increasing Reynolds number. The average error is about 19.6%. Fig. 5(b) shows the comparison of the friction factor. It can be seen that the numerical results have the similar tendency with the experimental results. The average relative error is about 20.9%. In summary, the numerical results can basically describe the heat transfer characteristics of the heat exchanger.

3. Establishment of reduced-order model

3.1 POD Sample selection

In the selection process of the sample, in order to capture the essential information of the physical problem as much as possible, the sampling condition can be determined by the method of “superposition of sample parameters”. Three parameters are selected in this study, they are transverse tube spacing, fin spacing and airflow velocity. Three samples are set up by changing single parameter, double parameters and three parameters. It should be noted that in the simulation of the heat transfer of the flat tube heat exchanger, the steady-state temperature field for different parameters is used as the sampling matrix. The specific parameters are shown in Table 2.

$$\begin{bmatrix} T(\xi_1, \eta_1, \zeta_1, c_i) \\ \vdots \\ T(\xi_I, \eta_1, \zeta_1, c_i) \\ T(\xi_1, \eta_2, \zeta_1, c_i) \\ \vdots \\ T(\xi_I, \eta_J, \zeta_1, c_i) \\ T(\xi_1, \eta_1, \zeta_2, c_i) \\ \vdots \\ T(\xi_1, \eta_J, \zeta_3, c_i) \\ \vdots \\ T(\xi_I, \eta_J, \zeta_K, c_i) \end{bmatrix} \Rightarrow \begin{bmatrix} T(\xi_1, \eta_1, \zeta_1, c_1) & T(\xi_1, \eta_1, \zeta_1, c_2) & \cdots & T(\xi_1, \eta_1, \zeta_1, c_{N-1}) & T(\xi_1, \eta_1, \zeta_1, c_N) \\ \vdots & \vdots & \cdots & \vdots & \vdots \\ T(\xi_I, \eta_1, \zeta_1, c_1) & T(\xi_I, \eta_1, \zeta_1, c_2) & \cdots & T(\xi_I, \eta_1, \zeta_1, c_{N-1}) & T(\xi_I, \eta_1, \zeta_1, c_N) \\ T(\xi_1, \eta_2, \zeta_1, c_1) & T(\xi_1, \eta_2, \zeta_1, c_2) & \cdots & T(\xi_1, \eta_2, \zeta_1, c_{N-1}) & T(\xi_1, \eta_2, \zeta_1, c_N) \\ \vdots & \vdots & \cdots & \vdots & \vdots \\ T(\xi_I, \eta_J, \zeta_1, c_1) & T(\xi_I, \eta_J, \zeta_1, c_2) & \cdots & T(\xi_I, \eta_J, \zeta_1, c_{N-1}) & T(\xi_I, \eta_J, \zeta_1, c_N) \\ T(\xi_1, \eta_1, \zeta_2, c_1) & T(\xi_1, \eta_1, \zeta_2, c_2) & \cdots & T(\xi_1, \eta_1, \zeta_2, c_{N-1}) & T(\xi_1, \eta_1, \zeta_2, c_N) \\ \vdots & \vdots & \cdots & \vdots & \vdots \\ T(\xi_I, \eta_J, \zeta_2, c_1) & T(\xi_I, \eta_J, \zeta_2, c_2) & \cdots & T(\xi_I, \eta_J, \zeta_2, c_{N-1}) & T(\xi_I, \eta_J, \zeta_2, c_N) \\ T(\xi_I, \eta_J, \zeta_3, c_1) & T(\xi_I, \eta_J, \zeta_3, c_2) & \cdots & T(\xi_I, \eta_J, \zeta_3, c_{N-1}) & T(\xi_I, \eta_J, \zeta_3, c_N) \\ \vdots & \vdots & \cdots & \vdots & \vdots \\ T(\xi_I, \eta_J, \zeta_K, c_1) & T(\xi_I, \eta_J, \zeta_K, c_2) & \cdots & T(\xi_I, \eta_J, \zeta_K, c_{N-1}) & T(\xi_I, \eta_J, \zeta_K, c_N) \end{bmatrix} \quad (12)$$

Table 2. Sample parameters.

Sample data	parameter name	single parameter	double parameters	three parameters
Variety parameter	Re	A	A	A
	T_p	2	B	B
	S_1	16	16	16
Number of samples		10	30	90

$A=\{200,400,600,800,1000,1200,1400,1600,1800,2000\}$ $B=\{1.6,2.0,2.4\}mm$ $C=\{12.8,16.0,21.2\}mm$

The relationship of sample and sample data can be illustrated in formula (12). Firstly, the temperature field of the unsteady heat transfer is calculated by FVM, then the proper samples are selected and the calculated temperature field is stored in the sample matrix. In formula (12), the single sample is listed on the left side, the right side represents the sample matrix and N is the total number of samples, the single sample on the left side can be expanded in the form of matrix as shown in the right side of formula (12). Where ξ, η, ζ are the body-fitted coordinates corresponding to the cartesian coordinate system.

All data of the temperature fields under all sample conditions can be written in the order as shown in formula (12). The sampling matrix is obtained by arranging all the vectors in order.

3.2 Basis function calculation

Although more basis functions are selected, the accuracy of the POD reduced-order model is not necessarily high, the corresponding calculation costs will increase. This situation is very significant in multi-sample, multi-parameter engineering practical problems. In this paper, the energy standard is used to select the basis function.

The obtained basis functions are arranged in order according to the energy of the samples. According to the number of samples of different sample matrices in Table 2, 10, 30 and 90 basis functions are obtained from the three sample matrices of single, double and three parameters. The basic trend of the temperature field distribution is described in the first basis function, the temperature field correction is emphasized in the second and third basis function. More and more detailed information was described with the increasing base function. Under normal circumstances, a high accuracy can be obtained by selecting about 10 basis functions in fixed shape region. Therefore, the first ten basis functions are chosen as the basis of the POD reduced-order model.

3.3 Proper interpolation method selection

The spectral coefficients of the unknown physical field can be obtained by interpolating the spectral coefficients of several known physical fields. Different interpolation methods were used to reconstruct the temperature field for different samples. In the case of single parameter variation samples, the Newton interpolation was chosen to calculate the interpolation spectral

coefficients. In the two-parameter variation sample calculation, cubic B-spline interpolation was selected to calculate and in the three-parameter variation sample calculation the linear interpolation was selected to calculate, respectively. The basic theory as to the interpolation method can be found in (Cao, 2012).

The specific interpolation formulas are as follows.

(1) Linear interpolation

Univariate linear interpolation of univariate Problems.

$$P_a = P_{a_1} + [P_{a_2} - P_{a_1}] \frac{a - a_1}{a_2 - a_1} \quad (13)$$

Binary linear interpolation of two variable problems,

$$P_{ab} = \frac{a - a_1}{a_2 - a_1} \left[\frac{b - b_1}{b_2 - b_1} (P_{a_1 b_1} + P_{a_2 b_2} - P_{a_2 b_1} - P_{a_1 b_2}) + P_{a_2 b_1} - P_{a_1 b_1} \right] + \frac{b - b_1}{b_2 - b_1} (P_{a_1 b_2} - P_{a_1 b_1}) + P_{a_1 b_1} \quad (14)$$

Three variables are the same as above.

(2) Newton interpolation

$$f(x) = f(x_0) + f[x_0, x_1](x_0 - x_1) + f[x_0, x_1, x_3, \dots, x_n] \cdot (x - x_0)(x - x_1) + \dots + f[x_0, x_1, x_3, \dots, x_n] \cdot (x - x_0)(x - x_1) \dots (x - x_{n-1}) + f[x_0, x_1, x_3, \dots, x_n] \cdot (x - x_0)(x - x_1) \dots (x - x_{n-1})(x - x_n) \quad (15)$$

Equation (15) is the Newton interpolation at point x . In this study, the Newton interpolation is used to obtain the spectral coefficients under univariate conditions.

(3) Lagrangian interpolation

The Lagrangian interpolation is more flexible than the Newton interpolation but it is easier to increase or decrease the node. In this study, the Lagrangian interpolation method is used to obtain the spectral coefficients under univariate conditions. The Lagrangian equations are defined as follows.

$$f(x_j) = y_j, j = 0, 1, \dots, n \quad (16)$$

$$L_n(x) = \sum_{i=1}^n y_i l_i(x) \quad (17)$$

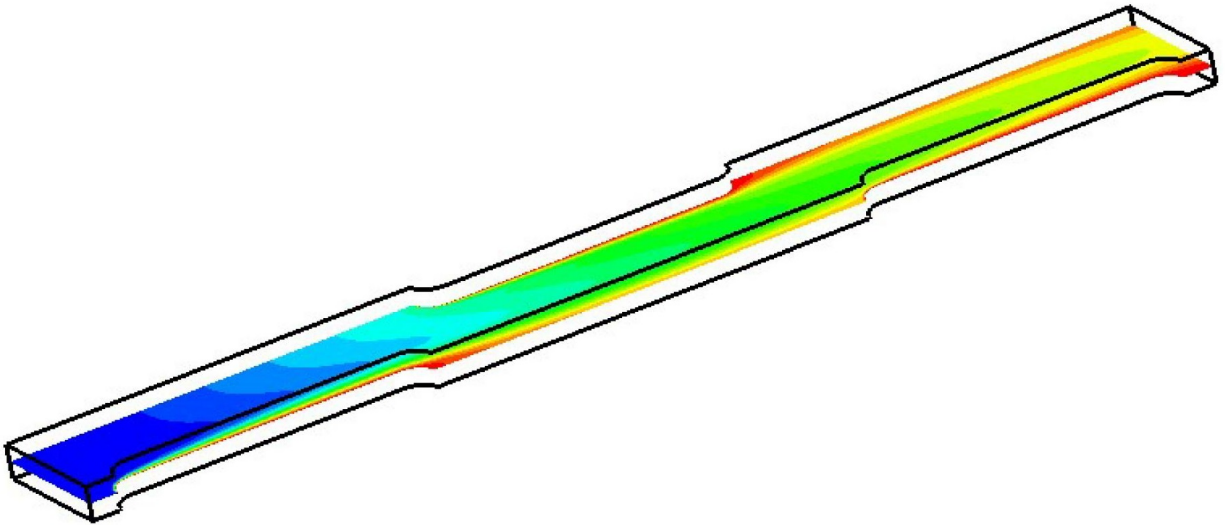


Fig. 6. Contrast plane in the calculate model.

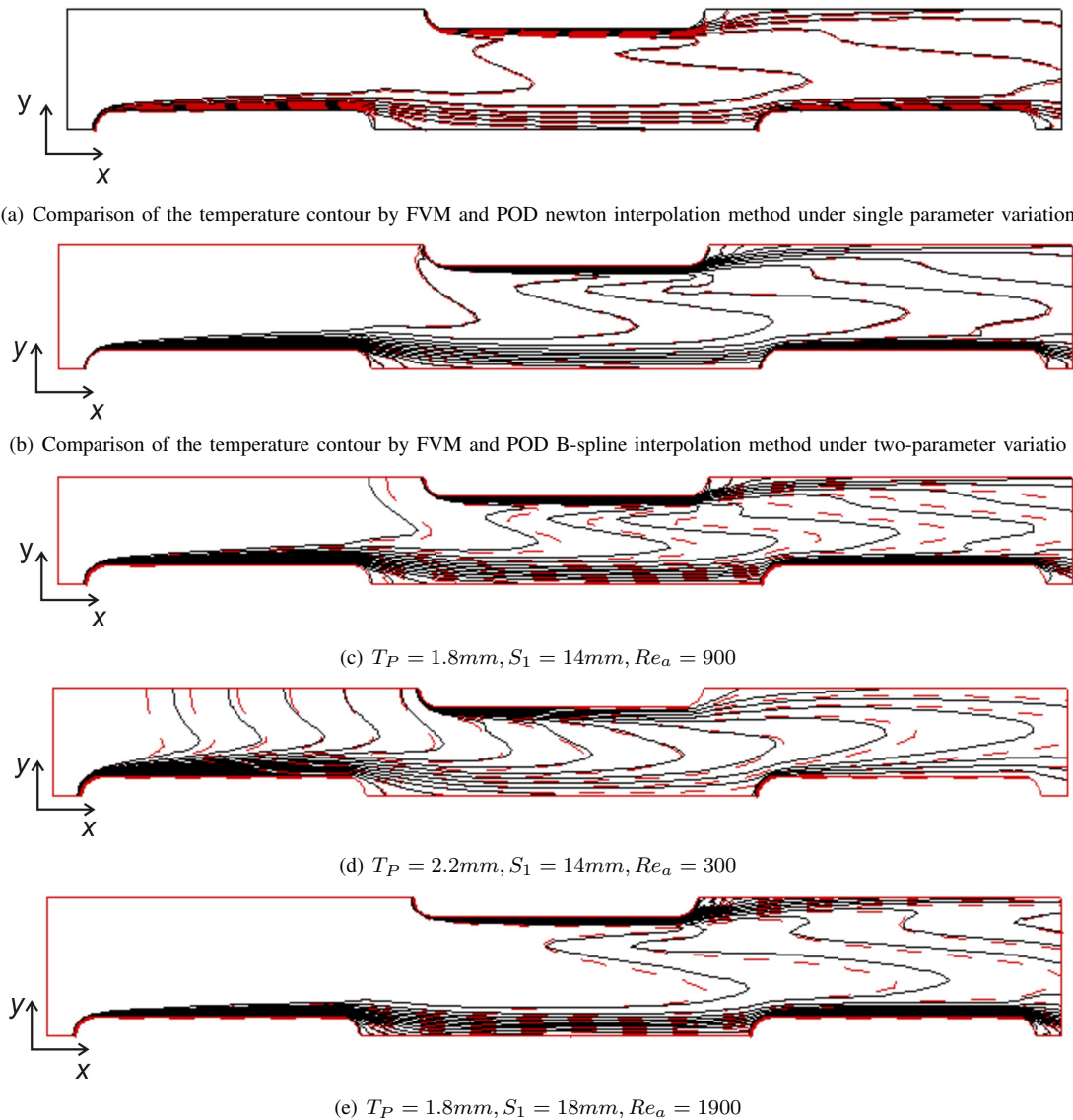


Fig. 7. Comparison of the temperature contour by FVM and POD.

$$l_i(x) = \frac{(x - x_0) \dots (x - x_{i-1})(x - x_{i+1}) \dots (x - x_n)}{(x_i - x_0) \dots (x_i - x_{i-1})(x_i - x_{i+1}) \dots (x_i - x_n)},$$

$$i = 0, 1, \dots, n \quad (18)$$

$$l_i(x_j) = \begin{cases} 1, & i = j \\ 0, & i \neq j \end{cases} \quad i, j = 0, 1, \dots, n \quad (19)$$

$$L_n(x_j) = y_j, j = 0, 1, \dots, n \quad (20)$$

Equation (18) is Lagrangian polynomial and the calculated interpolation is the Lagrangian polynomial interpolation.

(4) Cubic B-spline interpolation

Cubic B-spline interpolation is a universal segmentation interpolation method which can avoid the oscillation problem of high order polynomials and guarantee the smoothness of the interpolation curve. The corresponding spectral coefficients are calculated by using cubic B-spline interpolation under univariate and bivariate conditions here (Ren, 2008).

4. Results and discussion

4.1 Reliability of the POD interpolation method

FVM, as a classical numerical heat transfer calculation method, has been widely recognized in scientific study. In order to test the calculation accuracy and calculation speed of the POD reduced-order model, the temperature field distribution of the two methods were compared on $z = T_p/2$ section as the Fig. 6.

Based on the spectral coefficients obtained by the above interpolation methods, the temperature field was calculated by the established POD reduced-order model. Three different parameters of the sample reconstruction results were analyzed and the appropriate difference methods with least error were selected. The Newton interpolation method was used to calculate the unknown physical field under the univariate condition, the B-spline interpolation method was used to calculate the unknown physical field under two-parameter variation condition and the linear interpolation method was used to calculate the unknown physical field under the three-parameter variation condition. The comparison of FVM results and POD results in three conditions are shown as follow. The black solid line presents FVM results and the red dotted line presents POD interpolation results.

The comparison of temperature field under the univariate condition (only Re_a) on $z = T_p/2$ section when $T_p = 2 \text{ mm}$, $S_1 = 16 \text{ mm}$ and $Re_a = 1100$ is obtained as Fig. 7(a).

The comparison of temperature field under two-parameter variation condition (Re_a and T_p) when $T_p = 2.2 \text{ mm}$, $S_1 = 16 \text{ mm}$ and $Re_a = 1500$ on $z = T_p/2$ section is obtained as Fig. 7(b).

The comparison of temperature field under the three-parameter variation condition (Re_a , T_p and S_1) on $z = T_p/2$ section is obtained as Fig. 7(c)-(e).

It can be seen from Fig. 7 that the three cases have different relative errors. The maximum error between the POD results and FVM results are shown in Table 3. The relative maximum

Table 3. The maximum error of FVM and POD results.

Cases	a	b	c	d	e
Maximum error	0.019%	1.18%	5.27%	4.96%	3.83%

error is between 0.019% and 5.27%. The error range is acceptable in engineering calculation.

4.2 Reconstruction temperature field by POD interpolation method

Based on the spectral coefficients obtained by the above interpolation methods, the fitted temperature field under different conditions was calculated by using the established POD reduced-order model. Three different parameters of the sample reconstruction results are analyzed as follow.

(1) Single parameter variation (only Re_a)

The Newton interpolation method was used to calculate the unknown physical field under the univariate condition on the $z = T_p/2$ section when $T_p = 2 \text{ mm}$, $S_1 = 16 \text{ mm}$ and $Re_a = 1100$. The temperature field is obtained as Fig. 8.

(2) Two-parameter variation (Re_a and T_p)

The B-spline interpolation method was used to calculate the unknown physical field under two-parameter variation condition when $T_p = 2 \text{ mm}$, $S_1 = 16 \text{ mm}$ and $Re_a = 1100$ on $z = T_p/2$ section. The temperature field is obtained as Fig. 9.

(3) Three-parameter variation (Re_a , T_p and S_1)

The linear interpolation method was used to calculate the unknown physical field when $T_p = 2.2 \text{ mm}$, $S_1 = 16 \text{ mm}$, $Re_a = 1500$ on $z = T_p/2$ section under the three-parameter variation condition. The temperature reconstruction field is obtained as Fig. 10.

4.3 Comparison of interpolation method and FVM

Table 4 shows the comparison of average time-consuming of the FVM of SIMPLE algorithm and three types of POD interpolation methods. They are linear interpolation, newton interpolation and B-spline interpolation. It is easy to see that the POD method reduces the computational time greatly than that of the traditional numerical calculating method. Thus, the physical fields reconstructed by POD interpolation method can be considered when the accuracy of the results is satisfied with the engineering requirements.

It is very important to choose a suitable numerical method that can accurately predict the heat transfer characteristics of the heat exchanger from viewpoint of design. The FVM of SIMPLE algorithm is usually used to calculate the approximation simulation field but the calculation program is always complex and spend a long time. The POD method used in this paper is superior in computational accuracy and speed. Considering the practical application, POD interpolation method proposed in this study is better than the FVM in terms of accuracy, suitability and computational speed, which provides

Table 4. Sample parameter table.

Calculation method	SIMPLE algorithm	Linear interpolation	Newton interpolation	B-spline interpolation
Time consumings	10003.98	4.92	6.24	60.71
Multiple	-	2033.3	1603.20	164.78

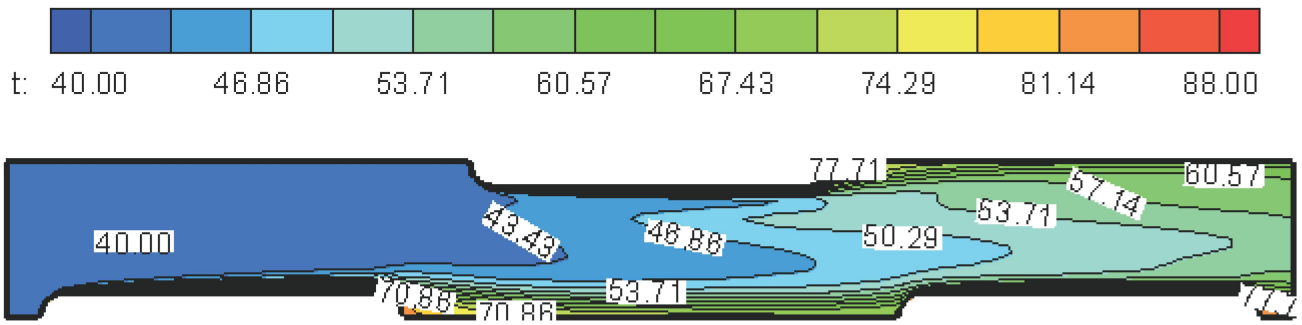


Fig. 8. Reconstruction temperature field by Newton interpolation method of univariate ($z = Tp/2$).

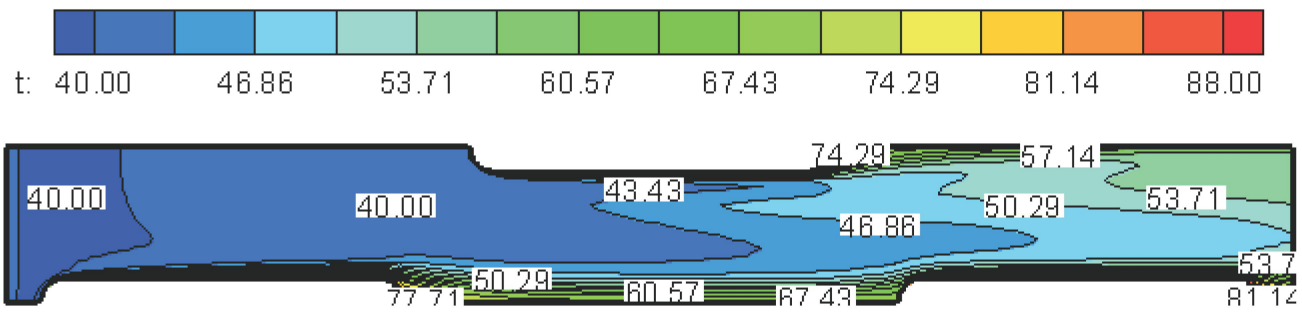


Fig. 9. Reconstruction temperature field by B-spline interpolation method of bivariate ($z = Tp/2$).

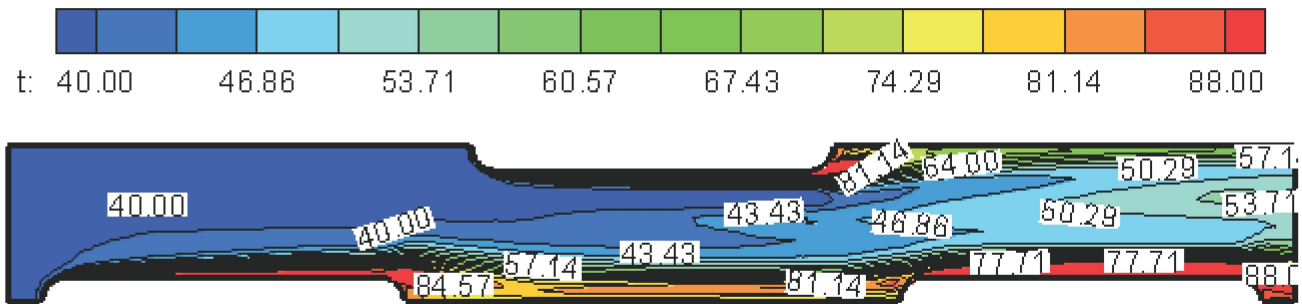


Fig. 10. Reconstruction temperature field by linear interpolation method under three-parameter variation conditions ($z = Tp/2$).

favorable conditions for the preheating, real-time monitoring and automatic control of the heat exchanger.

5. Conclusions

In this paper, the heat transfer of the flat tube bank fin heat exchanger was simulated. Firstly, the FVM was used to analyze the temperature field of the air side of the flat tube bank fin heat exchanger at different Reynolds numbers, fin spacing and different transverse tube spacing. The sampling matrix was obtained by the calculating results. Secondly, the basis function was obtained by decomposing the sampling matrix with SVD. Finally, different POD interpolation methods were used to reconstruct the temperature field and the reconstruction temperature fields were compared with the FVM results. The main conclusions are as follows.

(1) In the study of the flat tube bank fin heat exchanger unit, the reconstructed temperature field conforming to the variation of the original temperature field can be calculated by POD interpolation method. It can be seen that the POD interpolation method can be applied to solve the multivariable steady-state problem of complex boundary conditions as the heat exchanger. The POD interpolation method is used to interpolate the spectral coefficients of the given samples to obtain the new spectral coefficients, which greatly simplifies the solution process. Though the accuracy of the calculation results is highly dependent on the interpolation method itself and the sample data, it is more advantageous in the calculation efficiency. Compared with the traditional numerical heat transfer SIMPLE algorithm, the POD reduced-order model proposed in this paper greatly improves the calculating speed, which can guarantee calculation precision and reduce the storage space of the computer.

(2) In the process of physical field reconstructed by POD interpolation method, different interpolation methods have different effects on the computational accuracy. Compared with the temperature field by FVM, the fitting curves of higher order linear interpolation and segmented interpolation have higher accuracy than that of linear interpolation. In general, the reconstructed temperature fields obtained by POD interpolation method are different from the original physical field.

(3) The POD is applied to heat transfer calculation of complex structure such as flat tube bank fin heat exchanger greatly expanded its engineering applications. However, this method should be explored continually. For example, it should be used to reconstruct the temperature and velocity field under the condition of conjugate heat transfer boundary conditions. In addition, the problem about flow and heat transfer in flat tube bank fin heat exchanger with vortex generators under more complex boundary condition may show the superiority of the POD reduced-order model.

Nomenclature

a =water pipe width [m]
 ρ =fluid density [kg/m^3]
 b =water pipe length [m]

u, v, w =velocity component [m/s]
 d_e =characteristic dimension [m]
 μ =dynamic viscosity [$Pa \cdot s$]
 f =friction factor
 ν =kinetic viscosity [m^2/s]
 L =characteristic length [m]
 a =thermal conductivity
 L_y =span-wise length of the fin [m]
 ε =discrepancy between the Nusselt numbers obtained by different numerical methods [-]
 Nu =Nusselt number
 λ =thermal conductivity [$W/(m \cdot k)$]
 Gr =Glashov number
 ξ, η, ζ =body fitted coordinator axes coordinator axes
 Pr =Prandtl number
 Re =Reynolds number [-]
 Ra =Rayleigh number [-]
 S_1 =transverse tube spacing [m]
 S_2 =longitudinal tube spacing [m]
 T_p =fin spacing [m]
 T_w =tube wall temperature [K]
 T =fluid temperature of the computational domain

Subscripts

a =air
 out =outlet
 a, b =non-sample parameters
 in =inlet
 a_1, b_1 =minimum sample interval
 w =wall or fin surface
 max =the maximum value
 fin =the fin of heat exchanger
 min =the minimum value

Acknowledgments

The study was supported by the National Science Foundation of China (Nos. 51476073, 51576210 and 51266004)

Open Access This article is distributed under the terms and conditions of the Creative Commons Attribution (CC BY-NC-ND) license, which permits unrestricted use, distribution, and reproduction in any medium, provided the original work is properly cited.

References

- Agbossou, A., Souyri, B., Stutz, B. Modelling of helical coil heat exchangers for heat pump applications: Analysis of operating modes and distance between heat exchangers. Appl. Therm. Eng. 2018, 129: 1068-1078.
- Aliabadi, M., Akbari, M., Hormozi, F. An empirical study on vortex-generator inset fitted in tubular heat exchanger with dilute Cu-water nanofluid flow. Chinese J. Chem. Eng. 2016, 24(6): 728-736.
- Aquino, W. An object-oriented framework for reduced-order models using proper orthogonal decomposition (POD). Comput. Method. Appl. M. 2007, 196(41): 4375-4390.
- Arora, A., Subbarao, P.M.V., Agarwal, R.S. Numerical optimization of location of 'common flow up' delta

- winglets for inline aligned finned tube heat exchangers. *Appl. Therm. Eng.* 2015, 82: 329-340.
- Atam, E., Helsen. Ground-coupled heat pumps: Part 1 - Literature review and research challenges in modeling and optimal control. *Renew. Sust. Energ. Rev.* 2016, 54: 1653-1667.
- Bellocchi, S., Guizzi, L., Manno, M., et al. Reversible heat pump HVAC system with regenerative heat exchanger for electric vehicles: Analysis of its impact on driving range. *Appl. Therm. Eng.* 2018, 129: 290-305.
- Brenner, T.A., Fontenot, R.L., Cizmas, P.G.A., et al. A reduced-order model for heat transfer in multiphase flow and practical aspects of the proper orthogonal decomposition. *Comput. Chem. Eng.* 2012, 43: 68-80.
- Cao, Y.H., Zhu, J., Luo, Z.D., et al. Reduced-order modeling of the upper tropical pacific ocean model using proper orthogonal decomposition. *Comput. Math. Appl.* 2006, 52(8-9): 1373-1386.
- Cao, Z.Z. Calculation of temperature field in POD method of hot oil pipeline. Beijing: China University of Petroleum, 2012 (in Chinese).
- Capata, R., Beyene, A. Experimental evaluation of three different configurations of constructal disc-shaped heat exchangers. *Int. J. Heat Mass Tran.* 2017, 115: 92-101.
- Cazemier, W., Verstappen, R.W.C.P., Veldman, A.E.P. Proper orthogonal decomposition and low-dimensional models for driven cavity flows. *Phys. Fluids* 1998, 10(7): 1685-1699.
- Chen, Y.Q., Zhang, L.N., Zhao, B.B. Application of singular value decomposition (SVD) in extraction of gravity components indicating the deeply and shallowly buried granitic complex associated with tin polymetallic mineralization in the Gejiu tin ore field, Southwestern China. *J. Appl. Geophys.* 2015, 123: 63-70.
- Crommelinand, D.T., Majda, A.J. Strategies for model reduction: comparing different optimal bases. *J. Atmos. Sci.* 2004, 61(17): 2306-2317.
- Dezan, D., Salviano, L., Yanagihara, J. Heat transfer enhancement and optimization of flat-tube multilouvered fin compact heat exchangers with delta-winglet vortex generators. *Appl. Therm. Eng.* 2016, 101: 576-591.
- Ding, P., Tao, W.Q. Reduced order modeling of fluid flow and heat transfer in tube-fin heat exchanger. *J. Chin. Univ. Pet.* 2011, 35(2): 137-140 (in Chinese).
- Fukunaga, K. Introduction to statistical recognition. Academic Press, 1990.
- Gai, X.P., Wang, L.B., Lin, Z.M., et al. Effects of the fins conductivity on heat transfer performance of the bank plain fin heat exchangers. *J. Lanzhou Jiaotong Univ.* 2010, 29(3): 55-61 (in Chinese).
- Guo, K.P., Zhang, N., Smith, R. Design optimization of multi-stream plate fin heat exchangers with multiple fin types. *Appl. Therm. Eng.* 2017, doi: 10.1016/j.applthermaleng.2017.11.099.
- Han, D.X., Yu, B., Wang, Y., et al. Fast thermal simulation of a heated crude oil pipeline with a BFC-based POD reduced-order model. *Appl. Therm. Eng.* 2015, 88: 217-229.
- Han, H., He, Y.L., Li, Y.S., et al. A numerical study on compact enhanced fin-and-tube heat exchangers with oval and circular tube configurations. *Int. J. Heat Mass Transfer* 2013, 65: 686-695.
- Hu, W.L., Su, M., Wang, L.B., et al. The optimum fin spacing of circle tube bank fin heat exchanger with vortex generators under the same front velocity. *Heat Mass Transfer* 2013, 49(9): 1271-1285.
- Hu, W.L., Wang, L.B., Guan, Y. The effect of transverse tube pitch on the thermal-hydrodynamic performance of a circular tube-plate-fin heat exchanger with fin-mounted vortex generators. *J. Enhanc. Heat Transf.* 2015, 22(3): 221-246.
- Jacobi, A.M., Shah, R.K. Air-side flow and heat transfer in compact heat exchangers: A discussion of enhancement mechanisms. *Heat Transfer Eng.* 1998, 19(4): 29-41.
- Jolliffe, I.T. Principal component analysis. New York: Springer, 2002.
- Kylikof, U. The cooling system of diesel locomotive. Moscow, Russian: Machine Construction Press, 1988 (in Russian).
- Li, H.R., Luo, Z.D., Chen, J. Numerical simulation based on POD for two dimensional solute transport problems. *Appl. Math. Model.* 2011, 35(5): 2489-2498.
- Li, K.J., Xue, W.P., Xu, C., et al. Optimization of ventilation system operation in office environment using POD model reduction and genetic algorithm. *Energ. Buildings* 2013, 67: 34-43.
- Lin, Z.M., Liu, C.P., Wang, L.B. Numerical study of fluid flow and heat transfer enhancement of circular tube bank fin heat exchanger with curved delta-winglet vortex generators. *Appl. Therm. Eng.* 2015, 88: 198-210.
- Lin, Z.M., Wang, L.B., Zhang, Y.H., et al. Numerical study on heat transfer enhancement of circular tube bank fin heat exchanger with interrupted annular groove fin. *Appl. Therm. Eng.* 2014, 73: 1465-1476.
- Liu, C.P., Lin, Z.M., Wang, L.B. Thermal boundary conditions on the cross sections normal to the main flow of fully developed convection in the tube with insert tape. *Numer. Heat TR. A-Appl.* 2014, 65(12): 1230-1253.
- Liu, S., Wang, L.B., Fan, J.F., et al. Tube transverse pitch effect on heat/mass transfer characteristics of flat tube bank fin mounted with vortex generators. *J. Heat Tran.* 2008, 130(6): 064502.
- Lizardi, J.J., Trevino, C., Mendez, F. The influence of the variable thermal conductivity of a vertical fin on a laminar-film condensation process. *Heat Mass Transfer* 2004, 40(5): 383-391.
- Lumley, J.L. The structure of inhomogeneous turbulent flows, Yaglom A M and Tatarski V I Ed. *Atmospheric Turbulence and Radio Wave Propagation*, Nauka, Moscow. 1967: 166-178.
- Luo, Z.D., Zhu, J., Wang, R., et al. Proper orthogonal decomposition approach and error estimation of mixed finite element methods for the tropical Pacific Ocean reduced gravity model. *Comput. Method. Appl. M.* 2007, 196(41): 4184-4195.
- Mahapatra, P.S., Chatterjee, S., Mukhopadhyay, A., et al. Proper orthogonal decomposition of thermally-induced

- flow structure in an enclosure with alternately active localized heat sources. *Int. J. Heat Mass Tran.* 2016, 94: 373-379.
- Majda, A.J., Timofeyev, I., Vanden-Eijnden, E. Systematic strategies for stochastic mode reduction in climate. *J. Atmos. Sci.* 2003, 60(14): 1705-1723.
- Misevičiūtė, V., Motuzienė, V., Valančius, K. The application of the pinch method for the analysis of the heat exchangers network in a ventilation system of a building. *Appl. Therm. Eng.* 2018, 129: 772-781.
- Mudunuru, M., Karra, S., Harp, D. Regression-based reduced-order models to predict transient thermal output for enhanced geothermal systems. *Geothermics* 2017, 70: 192-205.
- Nair, H.C., Padmalal, D., Joseph, A. et al. Delineation of groundwater potential zones in river basins using geospatial tools an example from southern Western Ghats, Kerala, India. *J. Geovis. Spati. Anal.* 2017, 1(1-2): 1-5.
- Pearson, K. On lines and planes of closest fit to systems of points in space. *Philos. Mag.* 1901, 2(11): 559-572.
- Polansky, J., Wang, M. Proper orthogonal decomposition as a technique for identifying two-phase flow pattern based on electrical impedance tomography. *Flow Meas. Instrum.* 2017, 53: 126-132.
- Puragliesi, R., Leriche, E. Proper orthogonal decomposition of a fully confined cubical differentially heated cavity flow at Rayleigh number $Ra = 10^9$. *Comput. Fluids* 2012, 61: 14-20.
- Ren, Y.J. Numerical analysis and realization of matlab. Chinese: Higher Education Press, 2008.
- Rosenfeld, A., Kak, A. Digital picture processing. New York: Academic Press, 1982.
- Salviano, L., Dezan, D., Yanagihara, J.I. Thermal-hydraulic performance optimization of inline and staggered fin-tube compact heat exchanger applying longitudinal vortex generators. *Appl. Therm. Eng.* 2016, 95: 311-329.
- Singer, M.A., Green, W.H. Using adaptive proper orthogonal decomposition to solve the reaction-diffusion equation. *Appl. Numer. Math.* 2009, 59(2): 272-279.
- Sirovich, L. Turbulent and dynamics of coherent structure: I-III. *Q. Appl. Math.* 1987, 45(3): 561-571.
- Sivasakthivel, T., Philippe, M., Murugesan, K., et al. Experimental thermal performance analysis of ground heat exchangers for space heating and cooling applications. *Renew. Energy* 2017, 113: 1168-1181.
- Song, K.W., Wang, Y., Wang, L.B., et al. Numerical study of the fin efficiency and a modified fin efficiency formula for flat tube bank fin heat exchanger. *Int. J. Heat Mass Tran.* 2011, 54(11): 2661-2672.
- Song, K.W., Xi, Z.P., Su, M., et al. Effect of geometric size of curved delta winglet vortex generators and tube pitch on heat transfer characteristics of fin-tube heat exchanger. *Exp. Therm. Fluid Sci.* 2017, 82: 8-18.
- Välíkangas, T., Singh, S., Sørensen, K., et al. Fin-and-tube heat exchanger enhancement with a combined herringbone and vortex generator design. *Int. J. Heat Mass Tran.* 2018, 118: 602-616.
- Wang, L.B., Lin, Z.M., Sun, K.J., et al. Transversal tube pitch effects on local heat transfer characteristics of the flat tube bank fin mounted vortex generators and their sensitivity to non-uniform temperature of the fin. *Front. Energy Power Eng. Chin.* 2010, 4(3): 333-345.
- Wang, S.M., Jian, G.P., Tong, X., et al. Effects of spacing bars on the performance of spiral-wound heat exchanger and the fitting of empirical correlations. *Appl. Therm. Eng.* 2018, 128: 1351-1358.
- Wang, Y., Wang, L.C., Lin, Z.M., et al. The condition requiring conjugate numerical method in study of heat transfer characteristics of tube bank fin heat exchanger. *Int. J. Heat Mass Tran.* 2012a, 55(9): 2353-2364.
- Wang, Y., Yu, B., Cao, Z.Z., et al. A comparative study of POD interpolation and POD projection methods for fast and accurate prediction of heat transfer problems. *Int. J. Heat Mass Tran.* 2012b, 55(17): 4827-4836.
- Wang, Y., Yu, B., Wu, X., et al. POD and wavelet analyses on the flow structures of a polymer drag-reducing flow based on DNS data. *Int. J. Heat Mass Tran.* 2012c, 55(17): 4849-4861.
- Wang, Y., Yu, B., Sun, S.Y. Fast prediction method for steady-state heat convection. *Chem. Eng. Technol.* 2012d, 35(4): 668-678.
- Wang, Y., Yu, B., Wu, X., et al. POD study on the mechanism of turbulent drag reduction and heat transfer reduction based on direct numerical simulation. *Prog. Comput. Fluid Dyn.* 2011, 11(3/4): 149-159.
- Wei, X.Q., Zhang, Y.H., Hu, W.L., et al. The fluid flow and heat transfer characteristics in the channel formed by flat tube and dimpled fin. *Int. J. Therm. Sci.* 2016, 104: 86-100.
- Yang, J.C., Li, F.C., Cai, W.H., et al. On the mechanism of convective heat transfer enhancement in a turbulent flow of nanofluid investigated by DNS and analyses of POD and FSP. *Int. J. Heat Mass Tran.* 2014, 78: 277-288.
- Zhang, X.H., Xiang, H. A fast meshless method based on proper orthogonal decomposition for the transient heat conduction problems. *Int. J. Heat Mass Tran.* 2015, 84: 729-739.